INTERNATIONAL JOURNAL FOR NUMERICAL METHODS IN FLUIDS
Int. J. Numer. Meth. Fluids 2009; **61**:780–795
Published online 4 December 2008 in Wiley InterScience (www.interscience.wiley.com). DOI: 10.1002/fld.1975

An efficient numerical solution for linear stability of circular jet: A combination of Petrov–Galerkin spectral method and exponential coordinate transformation based on Fornberg's treatment

M. L. Xie[1] and J. Z. Lin[2,*,†]

[1]*The State Key Laboratory of Coal Combustion, Huazhong University of Science and Technology, Wuhan 430074, China*
[2]*China Jiliang University, Hangzhou 310018, China*

SUMMARY

This paper presents the linear stability analysis of a round jet in a radially unbounded domain using a spectral Petrov–Galerkin scheme coped with exponential coordinate transformation based on Fornberg's treatment. A Fourier–Chebyshev Petrov–Galerkin spectral method is described for the computation of the linear stability equations based on half a Gauss–Lobatto mesh. Complex basis functions presented here are exponentially mapped as Chebyshev functions, which satisfy the pole condition exactly at the origin, and can be used to expand vector functions efficiently by using the solenoidal condition. The mathematical formulation is presented in detail focusing on the solenoidal vector field used for the approximation of the flow. The scheme provides spectral accuracy in the present cases and the numerical results are in agreement with former works. Copyright © 2008 John Wiley & Sons, Ltd.

Received 5 June 2008; Revised 28 October 2008; Accepted 28 October 2008

KEY WORDS: hydrodynamic stability; circular jet; cylindrical system singularity; coordinate transformation; spectral Petrov–Galerkin scheme; projection method

1. INTRODUCTION

Jets are important in many practical applications, e.g. related to combustion, propulsion, mixing and aeroacoustics. As one of the generic flows of fluid mechanics, jets have been of scientific interest for over a 100 years [1]. The round jet results when fluid is emitted, with a given initial momentum, out of a circular orifice into a large space. At sufficiently high Reynolds number, this

*Correspondence to: J. Z. Lin, China Jiliang University, Hangzhou 310018, China.
†E-mail: mecjzlin@zju.edu.cn

Contract/grant sponsor: National Natural Science Foundation of China; contract/grant numbers: 50806023, 10632070, 50721005

jet will be turbulent. The stability properties of the flow play a fundamental role in the transition to turbulence and the formation of coherent vortex structures in a turbulent fluid [2, 3].

Frequently, the choice of independent variables is motivated by the symmetry of the circular jet; cylindrical coordinates are most appropriate. However, the choice of a particular set of independent variables might inadvertently introduce mathematically allowable, but physically unrealistic terms, e.g. singularities, which can decrease the accuracy or computational efficiency. Physically, the flow is continuous and regular at the axis [4]. These non-physical terms must be eliminated by the imposition of constraints on the mathematical solutions. The strategy to deal with this difficulty in analytical approaches is commonly that of discarding the singular solutions among all the admissible ones [5] (e.g. using Bessel's functions of the first kind and discarding those of the second kind [6]).

The treatment of the geometrical singularity in cylindrical and spherical coordinates has been a difficulty in the development of accurate finite difference (FD) and pseudo-spectral schemes for many years [7]. A variety of numerical procedures for dealing with the singularity have been suggested. The use of a spectral representation is often to be preferred for the accurate solution of problems with simple geometry [8–11]. In this case, the three-dimensional mathematical problem is transformed into a number of coupled two-dimensional ones for the spectral harmonics on the meridian plane. However, each of such problems is characterized by the singular terms whose degree of singularity grows with the harmonics. This is reflected by the number of regularity and boundary conditions that must be satisfied at the singular axis to allow a well-posed problem. Lopez *et al*. [12] derived regularity conditions by using the properties at the axis of the functions chosen to expand velocity and pressure along the radial direction, in which the radial and azimuthal components of the velocity are replaced by two complex functions. Pole conditions for Poisson-type equations in physical space were derived by Huang and Sloan [13]. Although they could solve the Poisson-type problems successfully, the time-step restriction problem that arises for advection problems due to the increased resolution near the coordinate singularity cannot be avoided. One way to avoid the time-step restriction is to use a Fourier filter in the azimuthal direction as used by Fornberg and Sloan [14] and Fornberg [15]. They used a Chebyshev expansion in the radial direction on $[-1, 1]$ over the coordinate singularity instead of on [0,1]. Their method avoids the time-step restriction problem and gives a good result for a simple linear advection problem. The merits of Fornberg's treatment in cylindrical geometries can also be found in the recent literature [16–19]. Priymak and Miyazakiy [20, 21] presented a robust numerical technique for the incompressible Navier–Stokes equations in cylindrical coordinates; the numerical solution is obtained using a spectral Galerkin method. Lopez and Shen [22] presented an efficient and accurate numerical scheme for the axisymmetric Navier–Stokes equations in primitive variables in a cylinder. The scheme is based on a new spectral Galerkin approximation for the space variables and a second-order projection scheme for the time variable. A sensible comparison is made with a standard second-order FD scheme based on a streamfunction-vorticity formulation. The numerical results indicated that both schemes produce very reliable results despite the singular boundary condition. The spectral projection scheme is still more accurate and more efficient than the FD scheme. More importantly, the spectral projection scheme can be readily extended to three dimensional, non-axisymmetric cases. Based on this method, Meseguer and Trefethen [23] described a Fourier–Chebyshev, Petrov–Galerkin spectral method for high accuracy computation of linearized flow in a finite circular pipe.

This paper considers the hydrodynamic stability of round jet flow in which there are no solid boundaries in the field. To construct a basis function set for unbounded domains, it is necessary to

DOI: 10.1002/fld

assume that the asymptotic behavior of the approximated functions for large r, as the approximated functions decay exponentially as r tends to infinity. There are many options for the basis functions. One way to treat this class of functions is the domain truncation method that imposes artificial boundary conditions at a sufficiently large radius [24]. The method can be made more efficient if additional mappings are used, so that standard spectral basis functions such as Chebyshev polynomials can be used. Grosch and Orszag [25] investigated the exponential and algebraic mapping methods in the semi-infinite domain and found by numerical experiments that the algebraic mapping gives a better result than the exponential mapping. Boyd [26] supported their result by examining the asymptotic behavior of the expansion coefficients of model functions by the method of steepest descent. Matsushima and Marcus [27] presented a spectral method for an unbounded domain using rational basis functions, which are algebraically mapped Legendre functions, and are used for the expansion in the radial direction of the polar coordinates. The method is not stiff when it is applied to initial-value problems despite the presence of the coordinate singularity. Solenoidal vector fields are treated efficiently by the toroidal and poloidal decomposition, which reduces the number of dependent variables from three to two.

In spite of these investigations cited above, the algebraic mapping has some drawbacks in the axisymmetric geometry, such as clustered points near the origin. But the use of an exponential mapping may treat the problem near the origin region easily. For example, an extra function can be included in the basis functions to represent the far-field behavior of the expanded functions more efficiently [28, 29]. In the present work, a spectral Petrov–Galerkin scheme for the numerical approximation of hydrodynamic stability equations in a circular jet is presented. The infinite domain is transformed into a finite unit disk domain by exponential mappings. In order to weaken the coordinate singularity at the axis, the discrete formulation of the disk with Chebyshev spectral method proposed by Fornberg and Sloan [14] is adopted. By restricting attention to solenoidal vector fields, the pressure variable is eliminated. Following [21–23], complex physical basis and test basis functions in a bounded domain are used for the expansion in the radial direction of polar coordinates. These functions satisfy the pole condition exactly at the coordinate singularity; they can be used in analytical studies and are particularly useful in numerical solutions. The numerical method is validated against the results available in the literature. The mathematical formulation and the exponential coordinate transformation are reported in Sections 2 and 3, respectively; the numerical solenoidal Petrov–Galerkin discretization method is derived in Section 4. Results and comparison with fifth-order variable step, Runge–Kutta method [5], compact FD method [30] and domain truncation method [24] in the literature are discussed in Section 5. Concluding remarks can be found in Section 6.

2. THE MATHEMATICAL FORMULATION

To derive the linearized equations for a round jet, we start with the incompressible dimensionless Navier–Stokes equations. These equations in cylindrical polar coordinates become

$$\frac{\partial u_r}{\partial r}+\frac{u_r}{r}+\frac{1}{r}\frac{\partial u_\theta}{\partial \theta}+\frac{\partial u_z}{\partial z}=0 \tag{1}$$

$$\frac{\mathrm{D}u_r}{\mathrm{D}t}-\frac{u_\theta^2}{r}=-\frac{1}{\rho}\frac{\partial p}{\partial r}+\frac{1}{Re}\left(\Delta u_r-\frac{u_r}{r^2}-\frac{2}{r^2}\frac{\partial u_\theta}{\partial \theta}\right) \tag{2}$$

DOI: 10.1002/fld

$$\frac{\mathrm{D}u_\theta}{\mathrm{D}t}+\frac{u_r u_\theta}{r}=-\frac{1}{\rho r}\frac{\partial p}{\partial \theta}+\frac{1}{Re}\left(\Delta u_\theta-\frac{u_\theta}{r^2}+\frac{2}{r^2}\frac{\partial u_r}{\partial \theta}\right) \tag{3}$$

$$\frac{\mathrm{D}u_z}{\mathrm{D}t}=-\frac{1}{\rho}\frac{\partial p}{\partial z}+\frac{1}{Re}\Delta u_z \tag{4}$$

where

$$\frac{\mathrm{D}}{\mathrm{D}t}\equiv\frac{\partial}{\partial t}+u_r\frac{\partial}{\partial r}+\frac{u_\theta}{r}\frac{\partial}{\partial \theta}+u_z\frac{\partial}{\partial z},\quad \Delta\equiv\frac{\partial^2}{\partial r^2}+\frac{1}{r}\frac{\partial}{\partial r}+\frac{1}{r^2}\frac{\partial^2}{\partial \theta^2}+\frac{\partial^2}{\partial z^2} \tag{5}$$

These equations are non-dimensionalized with respect to a length scale L_*, a velocity scale U_* and the Reynolds number $Re=L_*U_*/v$. The length scale and velocity scale are usually based on the jet core velocity and momentum thickness. Our concern in this paper is the linearized problem in which only infinitesimal perturbations from the laminar flow are considered, Let

$$u_r=U_r+u_r',\quad u_\theta=U_\theta+u_\theta',\quad u_z=U_z+u_z',\quad p=P+p' \tag{6}$$

and the perturbation can be expressed as superposition of complex Fourier modes of the form

$$\frac{u_r'}{u_r(r)}=\frac{u_\theta'}{u_\theta(r)}=\frac{u_z'}{u_z(r)}=\frac{p'}{\rho p(r)}=\mathrm{e}^{\mathrm{i}(n\theta+kz-\beta t)}=\mathrm{e}^{\mathrm{i}(n\theta+kz-kct)} \tag{7}$$

where $u_r(r)$, $u_\theta(r)$, $u_z(r)$ and $p(r)$ are the amplitudes of the corresponding disturbances, n is the azimuthal mode of the disturbance, k is the axial wavenumber of the disturbance, c (or $\beta=kc$) is the wave amplification factor. Then the linearized Navier–Stokes equations become

$$-\mathrm{i}kcu_r=-\mathrm{D}p+\frac{1}{Re}\left(\mathrm{D}^2u_r+\frac{1}{r}u_r-\frac{n^2+1}{r^2}u_r-k^2u_r-\frac{2}{r^2}\mathrm{i}nu_\theta\right)-\mathrm{i}kU_zu_r \tag{8}$$

$$-\mathrm{i}kcu_\theta=-\frac{\mathrm{i}n}{r}p+\frac{1}{Re}\left(\mathrm{D}^2u_\theta+\frac{1}{r}u_\theta-\frac{n^2+1}{r^2}u_\theta-k^2u_\theta+\frac{2}{r^2}\mathrm{i}nu_r\right)-\mathrm{i}kU_zu_\theta \tag{9}$$

$$-\mathrm{i}kcu_z=-\mathrm{i}kp+\frac{1}{Re}\left(\mathrm{D}^2u_z+\frac{1}{r}u_z-\frac{n^2}{r^2}u_z-k^2u_z\right)-u_r\mathrm{D}U_z-\mathrm{i}kU_zu_z \tag{10}$$

$$\left(\mathrm{D}+\frac{1}{r}\right)u_r+\mathrm{i}\left(\frac{1}{r}nu_\theta+ku_z\right)=0 \tag{11}$$

where $\mathrm{D}=\mathrm{d}/\mathrm{d}r$. The linear stability equations (8)–(11) are of singular Sturm–Liouville equation and have regular singularities at $r=0$.

In order to solve the linear system we must define the boundary conditions. According to Morris [31], the boundary conditions at the centerline of the jet are set for different azimuthal modes. In addition, in the far field, the boundary conditions are such that $\theta\to 0$ when $r\to\infty$. In particular, for each mode we must implement the following boundary conditions once the system has been defined and before the eigenvalue problem is solved. The following boundary conditions of disturbance were first derived by Batchelor and Gill [6], and then adopted by many researchers [32]. The

DOI: 10.1002/fld

boundary conditions take the form:

Case $n \neq 1$:

$$u_r(0) = u_\theta(0) = \mathrm{D}u_z(0) = \mathrm{D}p(0) = 0, \quad u_r(\infty) = u_\theta(\infty) = u_z(\infty) = p(\infty) = 0 \tag{12a}$$

Case $n = 1$:

$$u_r(0) + u_\theta(0) = \mathrm{D}u_z(0) = \mathrm{D}p(0) = 0, \quad u_r(\infty) = u_\theta(\infty) = u_z(\infty) = p(\infty) = 0 \tag{12b}$$

The mode of $n = 0$ is not considered in the present study in that the linear stability problem of a round jet reduces to the ordinary Orr–Sommerfeld equation. The first azimuthal mode disturbance ($n = 1$) is usually more unstable than the other azimuthal mode disturbance, and is the main object of the present study.

3. COORDINATE TRANSFORM

We investigate the utility of mappings to numerically solve the linear stability problem of a round jet in infinite regions. The numerical solution of continuum problems in unbounded regions involves two essential approximations: first, the continuum must be approximated by a discrete set and second, the unbounded domain must be approximated by a finite domain. The first problem is the one usually studied in numerical analysis. In order to have spectral accuracy in the numerical approximation, Chebyshev series is adopted in the present paper. The second problem in the present study is treated by a coordinate transformation of the infinite domain into a finite domain.

Spectral computations are frequently carried out in the bounded domains. The most common way to discretize the polar coordinates spectrally is to take a periodic Fourier grid in the azimuthal direction and a non-periodic Chebyshev grid in the radial component. Specifically, the grid in the radial direction is transformed from the usual Chebyshev grid for $x \in [-1, 1]$ by $x' = (x+1)/2$. The result is a polar grid that is highly clustered near both the boundary and the origin. Grids like this are convenient and commonly used, but they have some drawbacks. One difficulty is that while it is sometimes advantageous to have points clustered near the boundary, it may be wasteful and is certainly inelegant to devote extra grid points to the very small region near the origin, if the solution is smooth. Another is that for time-dependent problems, these small cells near the origin may force one to use excessively small time steps for numerical stability. Accordingly, various authors have found alternative ways to treat the region near the origin. In this paper we use the formulation proposed by Fornberg and Sloan [14, 15]. Closely related methods for polar coordinates have been used by others over the years; for a table summarizing twenty contributions in this area, see [26]. The idea is to take $x \in [-1, 1]$ instead of $x \in [0, 1]$. To expand this class of functions, we consider the exponential mapping

$$x = \frac{1 - \mathrm{e}^{-r/L}}{1 + \mathrm{e}^{-r/L}}, \quad r \in (-\infty, \infty) \quad \text{or} \quad r/L = \ln \frac{1+x}{1-x}, \quad x \in (-1, 1) \tag{13}$$

where $L > 0$ is the map parameter. The interval $-\infty < r < \infty$ is mapped to $-1 < x < 1$ on which the Chebyshev functions are orthogonal. In Figure 1 we plot x versus r for the exponential map with various values of L. The points indicate that the equivalent mesh in r is non-uniform with the most rapid variation occurring with $r \gg L$. The exponential map gives a good resolution near axis and it is especially useful in the treatment of the geometrical singularity for cylindrical coordinates. The map gives a better solution as $r \to \infty$ for larger parameter value of L.

DOI: 10.1002/fld

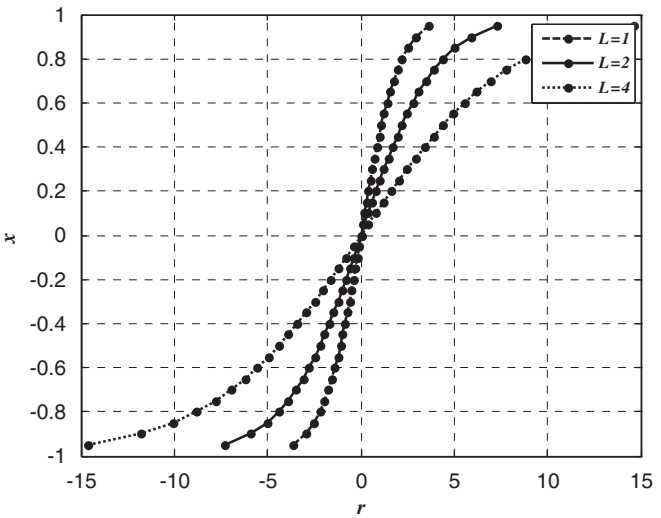

Figure 1. Variation of r versus x for the exponential map with various values of L.

Then the distribution of velocity in the round jet is [2]:

$$U_z = \frac{1}{(1+r^2)^2} = \frac{1}{(1+L^2 \ln^2(1+x)/(1-x))^2}, \quad x \in (-1, 1) \tag{14}$$

The exponential map is especially convenient because it yields simple expressions for derivatives. The derivatives with respect to r become:

$$\frac{\partial u}{\partial r} = \frac{1-x^2}{2L}\frac{\partial u}{\partial x}, \quad \frac{\partial^2 u}{\partial r^2} = \frac{1-x^2}{2L}\frac{\partial}{\partial x}\frac{1-x^2}{2L}\frac{\partial u}{\partial x} \tag{15}$$

The profile of the axial component of velocity of the round jet and its derivative for various values of L is shown in Figure 2. The larger the L, the sharper the profiles curve near the origin and a highly clustered grid is needed if the solution is smooth there. It may be wasteful and inelegant in the computation. Thus a smaller L is needed to save the cost of computation. Comparing Figures 2 and 3 with Figure 1, there is a contradiction in the choice of the map parameter L, and the problem is discussed and solved in Section 5.2.

We use Chebyshev series to represent the scalar function $u(r)$, then

$$u(x) = \sum_{j=0}^{N} a_j T_{2j}(x) \tag{16}$$

Here $T_{2j}(x)$ is the Chebyshev polynomial of degree j defined by

$$T_{2j}(\cos\theta) = \cos 2\mathrm{j}\theta \tag{17}$$

the set of $T_{2j}(x)$ for fixed integer j is complete and orthogonal with respect to weight function

$$w = 1/\sqrt{1-x^2} \tag{18}$$

DOI: 10.1002/fld

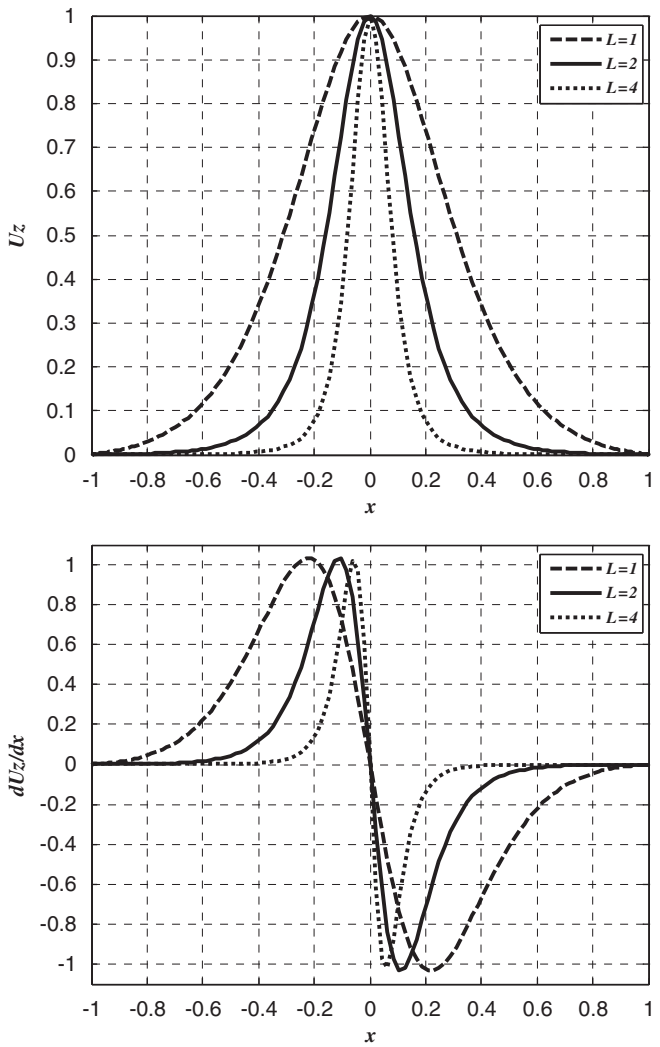

Figure 2. Distribution of axial component velocity and its derivation of round jet with various L.

The details of the application of Chebyshev series to the numerical solution of ordinary and partial differential equations are given in [33]. Then the linearized Navier–Stokes equations become

$$-\mathrm{i}kcu_r = -\mathrm{D}_* p + \frac{1}{Re}\left(\mathrm{D}_*^2 u_r + \frac{1}{r}u_r - \frac{n^2+1}{r^2}u_r - k^2 u_r - \frac{2}{r^2}\mathrm{i}nu_\theta\right) - \mathrm{i}kU_z u_r \tag{19}$$

$$-\mathrm{i}kcu_\theta = -\frac{\mathrm{i}n}{r}p + \frac{1}{Re}\left(\mathrm{D}_*^2 u_\theta + \frac{1}{r}u_\theta - \frac{n^2+1}{r^2}u_\theta - k^2 u_\theta + \frac{2}{r^2}\mathrm{i}nu_r\right) - \mathrm{i}kU_z u_\theta \tag{20}$$

DOI: 10.1002/fld

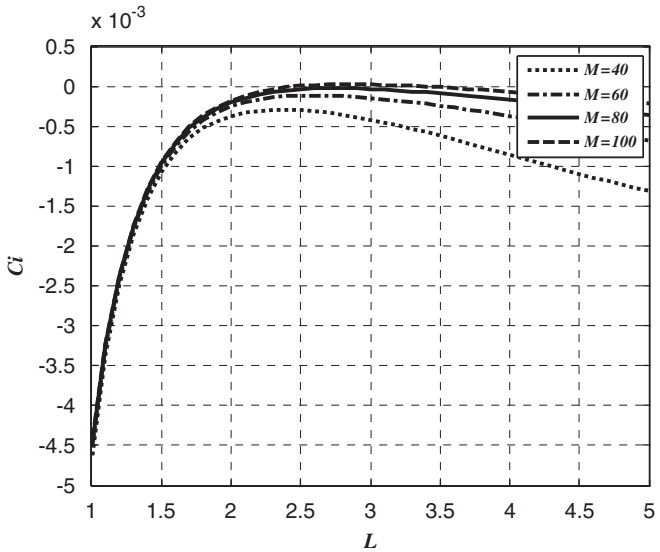

Figure 3. The effect of the Chebyshev polynomial order.

$$-\mathrm{i}kcu_z = -\mathrm{i}kp + \frac{1}{Re}\left(\mathrm{D}_*^2 u_z + \frac{1}{r}u_z - \frac{n^2}{r^2}u_z - k^2 u_z\right) - u_r \mathrm{D}_* U_z - \mathrm{i}kU_z u_z \tag{21}$$

$$\left(\mathrm{D}_* + \frac{1}{r}\right)u_r + \mathrm{i}\left(\frac{1}{r}nu_\theta + ku_z\right) = 0 \tag{22}$$

where $\mathrm{D}_* = (1-x^2)(\partial u/\partial x)/2L, r = L\ln(1+x)/(1-x)$. The boundary conditions of $n=1$ mode become:

$$u_r(0) + u_\theta(0) = \mathrm{D}u_z(0) = \mathrm{D}p(0) = 0, \quad u_r(1) = u_\theta(1) = u_z(1) = p(1) = 0 \tag{23}$$

4. SOLENOIDAL PETROV–GALERKIN DISCRETISATION

In order to have spectral accuracy in the numerical approximation of the eigenvalues problem, analyticity of the vector fields is required in the interval [0,1]. Transformations to polar coordinates are singular at $r=0$, making necessary a special treatment of our solution functions in a neighborhood of the origin. At this point, we must think of a complex variable problem instead of a real one. The domain of our problem is $|x| \leqslant 1$. The analyticity of the vector fields in the polar axis is ensured provided that the components satisfy the following property.

Theorem (Priymak and Miyazaki [21])
Consider a vector field $\mathbf{u}(r,\theta) = \mathrm{e}^{\mathrm{i}n\theta}[u_r(r)\mathbf{e}_r + u_\theta(r)\mathbf{e}_\theta + u_z(r)\mathbf{e}_z]$ for $r \leqslant \varepsilon$ for some $\varepsilon > 0$. The radial, azimuthal and axial components of $\mathbf{u}$ must satisfy the following conditions: $u_r(r) = rf_E(r)$, $u_\theta(r) = rg_E(r)$ for $n=0$ and $u_r(r) = r^{n-1}f_E(r)$, $u_\theta(r) = r^{n-1}g_E(r)$ for $n \neq 0$ for the radial and

DOI: 10.1002/fld

azimuthal components, and $u_z(r)=r^n h_E(r)$ for the axial component, where $f_E(r)$, $g_E(r)$ and $h_E(r)$ are functions that are analytic and even.

According to the regularity analysis of Priymak and Miyazaki [21] and Meseguer and Trefethen [23], the solenoidal solutions satisfy the conditions of the theorem. In addition, a straightforward Frobenius method provides the right parity conditions required by this theorem. In fact, Equations (19)–(21) are Bessel-type differential equations. Therefore, for n even, n^2 is also even, but n^2+1 is odd, u_z being an even function. By the same rule, u_r and u_θ are odd functions. The same reasoning can be applied for n odd. Our main goal is to approximate the solutions of the eigenvalues problem (19)–(22) by a spectral expansion. After substitution of the spectral expansion in the eigenvalues problem, the linearized operator is projected over another subspace of divergence-free fields (the dual or test space). Therefore, two different sets of vector fields are needed, one for the physical or trial space (noted as $\mathbf{u}_m$), and the other for the dual or test space (noted as $\mathbf{w}_m$), both solenoidal. There are many different ways of obtaining divergence-free fields in polar coordinates; we proceed in the way similar to that of Meseguer and Trefethen [23]. The solenoidal condition (22) introduces a linear dependence between the components, $u_r(r)$, $u_\theta(r)$, $u_z(r)$; therefore, there are only two degrees of freedom. The solenoidal basis for the approximation of the perturbation vector field takes the form

$$\mathbf{u}=\mathrm{e}^{\mathrm{i}(kz+n\theta-kct)}\sum_{m=0}^{M} a_m^{(1)}\mathbf{w}_m^{(1)}(x)\cdot\mathbf{u}_m^{(1)}(x)+a_m^{(2)}\mathbf{w}_m^{(2)}(x)\cdot\mathbf{u}_m^{(2)}(x) \tag{24}$$

which satisfy the analyticity and parity conditions. The vector fields $\mathbf{u}_m^{(1)}$ and $\mathbf{u}_m^{(2)}$ satisfy the zero divergence condition:

$$\nabla\cdot\mathrm{e}^{\mathrm{i}(kz+n\theta-kct)}\mathbf{u}_m^{(1,2)}=0 \tag{25}$$

In order to identify radial, azimuthal and axial component, the matrix notation is used:

$$\mathbf{u}_m^{(1,2)}=u_r\mathbf{e}_r+u_\theta\mathbf{e}_\theta+u_z\mathbf{e}_z=\begin{pmatrix}u_r\\u_\theta\\u_z\end{pmatrix} \tag{26}$$

Regarding the explicit solenoidal condition for $n\neq 0$:

$$\left(\mathrm{D}_*+\frac{1}{r}\right)u_r+\mathrm{i}\left(\frac{1}{r}nu_\theta+ku_z\right)=0 \tag{27}$$

There is a linear dependence between the components of the vector field. In this case, rendering the azimuthal or radial one free, any element of this subspace with order m can be expressed in the form

$$\mathbf{u}_m(x)=\mathrm{e}^{\mathrm{i}(kz+n\theta-kct)}[a_m^{(1)}\mathbf{u}_m^{(1)}(x)+a_m^{(2)}\mathbf{u}_m^{(2)}(x)] \tag{28}$$

in which the vector fields $\mathbf{u}_m^{(1)}$ and $\mathbf{u}_m^{(2)}$ take the form

$$\mathbf{u}_m^{(1)}(x)=\begin{pmatrix}-\mathrm{i}nu_r(x)\\ r\mathrm{D}_+[u_r(x)]\\0\end{pmatrix},\quad \mathbf{u}_m^{(2)}(x)=\begin{pmatrix}0\\-\mathrm{i}kru_\theta(x)\\ \mathrm{i}nu_\theta(x)\end{pmatrix} \tag{29}$$

DOI: 10.1002/fld

where $D_+ = D_* + 1/r$. Mathematically speaking, the factor of i in $u_m^{(2)}$ could be dispensed with; it is left in so that the basis functions have a desirable symmetry property. Then the aim is now to find suitable functions u_r and u_θ such that the conditions of theorem as well as homogenous boundary conditions are satisfied. For the azimuthal component we consider

$$u_\theta(x) = r^{n-1} h_m(x), \quad h_m(x) = (1-x^2) T_{2m}(x) \tag{30}$$

In the definition of the function $h_m(r)$, $T_{2m}(r)$ stands for the Chebyshev polynomial of order $2m$. The factor $(1-x^2)$ is added to make the vector field vanish over the wall. The factor x is necessary so that the analyticity conditions of the theorem are satisfied at the origin. We proceed in the same way for the radial component.

$$u_r(x) = r^n g_m(x), \quad g_m(x) = (1-x^2) h_m(x) \tag{31}$$

In this case the binomial $(1-x^2)$ is squared because the axial component also must vanish at $x = 1$. Then the physical or trial basis is:

$$\mathbf{u}_m^{(1)} = \begin{pmatrix} -\mathrm{i}n r^{n-1} g_m(x) \\ D_*[r^n g_m(x)] \\ 0 \end{pmatrix}, \quad \mathbf{u}_m^{(2)} = \begin{pmatrix} 0 \\ -\mathrm{i}k r^{n+1} h_m(x) \\ \mathrm{i}n r^n h_m(x) \end{pmatrix} \tag{29*}$$

We consider here the projection procedure in which the radial integration is involved. The radial Hermitian product is defined by the volume integral

$$(\mathbf{w}_m, \mathbf{u}_m) = \int_0^1 (\mathbf{w}_m^* \cdot \mathbf{u}_m) x \, \mathrm{d}x = \frac{1}{2} \int_{-1}^1 (\mathbf{w}_m^* \cdot \mathbf{u}_m) x \, \mathrm{d}x \tag{32}$$

where $\mathbf{u}_m$ belongs to the physical or trial space and $\mathbf{w}_m$ is a solenoidal vector field that belongs to the test or projection space. In order to take advantage of the orthogonality properties of Chebyshev polynomials, the test functions should be built up suitably. In essence, the projection fields are going to have the same structure as the trial fields, but the functions will be modified by the Chebyshev weight $(1-x^2)^{-1/2}$. However, the resulting matrices would be dense. They can be made to be bounded if the projection velocity fields are as follows:

$$\mathbf{w}_m^{(1)} = \frac{1}{\sqrt{1-x^2}} \begin{pmatrix} -\mathrm{i}n r g_m(x) \\ D_*[r^2 g_m(x)] + r^3 h_m(x) \\ 0 \end{pmatrix}, \quad \mathbf{w}_m^{(2)} = \frac{1}{\sqrt{1-x^2}} \begin{pmatrix} 0 \\ -\mathrm{i}k r^3 h_m(x) \\ \mathrm{i}n r^2 h_m(x) \end{pmatrix} \tag{33a}$$

for n odd, except that if $k = 0$, the third component of $\mathbf{w}_m^{(2)}$ is replaced by $r h_m(x)$, or

$$\mathbf{w}_m^{(1)} = \frac{1}{\sqrt{1-x^2}} \begin{pmatrix} -\mathrm{i}n g_m(x) \\ D_*[r g_m(x)] + r^2 h_m(x) \\ 0 \end{pmatrix}, \quad \mathbf{w}_m^{(2)} = \frac{1}{\sqrt{1-x^2}} \begin{pmatrix} 0 \\ -\mathrm{i}k r^2 h_m(x) \\ \mathrm{i}n r h_m(x) \end{pmatrix} \tag{33b}$$

for n even, except that if $k = 0$, the third component of $\mathbf{w}_m^{(2)}$ is replaced by $h_m(x)$.

The right-hand side integral in Equation (33) can be computed exactly by Gauss–Chebyshev–Lobatto quadrature formulas. In fact, the even form of the integrand will be used in order to avoid

DOI: 10.1002/fld

unnecessary computations. We will only consider half a Gauss–Lobatto mesh. From this point of view, analyticity imposes some restrictions that can be used to optimize the computational cost.

The Petrov–Galerkin projection scheme is carried out by substituting the spectral approximation in equations and projecting over the dual space. This procedure leads to a discretized generalized eigenvalues problem, and the coefficient $a_m^{(1,2)}$ governs the temporal behavior of the perturbation.

$$\begin{bmatrix} (\mathbf{w}_m^{(1)} \cdot \ell[\mathbf{u}_m^{(1)}]) & (\mathbf{w}_m^{(1)} \cdot \ell[\mathbf{u}_m^{(2)}]) \\ (\mathbf{w}_m^{(2)} \cdot \ell[\mathbf{u}_m^{(1)}]) & (\mathbf{w}_m^{(2)} \cdot \ell[\mathbf{u}_m^{(2)}]) \end{bmatrix} \begin{bmatrix} a_m^{(1)} \\ a_m^{(2)} \end{bmatrix} = c \begin{bmatrix} (\mathbf{w}_m^{(1)} \cdot \mathbf{u}_m^{(1)}) & (\mathbf{w}_m^{(1)} \cdot \mathbf{u}_m^{(2)}) \\ (\mathbf{w}_m^{(2)} \cdot \mathbf{u}_m^{(1)}) & (\mathbf{w}_m^{(2)} \cdot \mathbf{u}_m^{(2)}) \end{bmatrix} \begin{bmatrix} a_m^{(1)} \\ a_m^{(2)} \end{bmatrix} \tag{34}$$

where ℓ stands for the linear operator of linear stability equations

$$\ell[\cdot] = \frac{1}{Re}\Delta[\cdot] - \mathbf{u}_\mathrm{B} \cdot \nabla[\cdot] - [\cdot] \cdot \nabla \mathbf{u}_\mathrm{B} \tag{35}$$

where $\mathbf{u}_\mathrm{B}$ are the basic flow velocity vector $(0, 0, U_z)$. The pressure term should be formally included in the operator ℓ, but it is cancelled when projecting it over $\mathbf{w}$, that is $(\mathbf{w}, \nabla p) = 0$, and where the Hermitian product is the volume integral

$$(\mathbf{w}, \nabla p) = \int_0^1 x \, \mathrm{d}x \int_0^{2\pi} \mathrm{d}\theta \int_0^{2\pi/k} (\mathbf{w}^* \cdot \nabla p) \, \mathrm{d}z \tag{36}$$

Symbolically, Equation (39) can be written as

$$A_{Re}(n, k)u = cB(n, k)u \tag{37}$$

where A_{Re} is a matrix that depends on the Reynolds number. In addition, the matrices A_{Re} and B depend on n and k, being decoupled for each pair of them. The explicit matrix elements of A_{Re} are provided by the Hermitian products

$$A_{Re}(n, k)_{ij} = \begin{bmatrix} (\mathbf{w}_i^{(1)} \cdot \ell[\mathbf{u}_j^{(1)}]) & (\mathbf{w}_i^{(1)} \cdot \ell[\mathbf{u}_j^{(2)}]) \\ (\mathbf{w}_i^{(2)} \cdot \ell[\mathbf{u}_j^{(1)}]) & (\mathbf{w}_i^{(2)} \cdot \ell[\mathbf{u}_j^{(2)}]) \end{bmatrix} \quad (0 \leqslant i, j \leqslant M) \tag{38a}$$

$$B(n, k)_{ij} = \begin{bmatrix} (\mathbf{w}_i^{(1)} \cdot \mathbf{u}_j^{(1)}) & (\mathbf{w}_i^{(1)} \cdot \mathbf{u}_j^{(2)}) \\ (\mathbf{w}_i^{(2)} \cdot \mathbf{u}_j^{(1)}) & (\mathbf{w}_i^{(2)} \cdot \mathbf{u}_j^{(2)}) \end{bmatrix} \quad (0 \leqslant i, j \leqslant M) \tag{38b}$$

Let M be the approximation orders of Chebyshev polynomial in the axial, azimuthal and radial coordinates, respectively. The matrix dimension of the linear system A_{Re} and B is $2(M+1)$. The following orthogonality relations are useful in order to take advantages of the azimuthal and axial symmetries:

$$\int_0^{2\pi} \mathrm{e}^{\mathrm{i}(n'-n)} \, \mathrm{d}\theta = 2\pi\delta_n^{n'} \int_0^{2\pi/k} \mathrm{e}^{\mathrm{i}(k'-k)z} \, \mathrm{d}z = \frac{2\pi}{k}\delta_k^{k'} \tag{39}$$

where δ_j^i is the Kronecker symbol. In the present study, the temporal instability of the round jet is considered. Hence, k and n are real quantities while $c = c_r + \mathrm{i}c_i$ is generally complex. The disturbances will grow with time if $c_i > 0$ and will decay $c_i < 0$ in Equation (7). The neutral disturbances are then characterized by $c_i = 0$.

DOI: 10.1002/fld

5. RESULTS AND DISCUSSION

In stability analysis the most important eigenvalue is the one that is the most unstable or least stable. For the present framework, this corresponds to the eigenvalue with the least imaginary part. In particular, the flow will be temporal unstable if the imaginary part of the complex amplification is positive. The results in the present section have been obtained by parametrically varying the Reynolds number and frequency for an azimuthal wave number n of 1.

5.1. The order of Chebyshev polynomial effect

The wave amplifications (c_i) of round jet for M ranging from 40 to 100 are shown in Figure 3. It shows that the wave amplification of a round jet at $M=80$ has almost the same trend as that of $M=100$. It can be concluded that $M=100$ is far away enough for the accuracy of wave amplifications. Hence, the order of Chebyshev polynomial is defined at $M=100$ in the present study.

5.2. The map parameter L effect

From the analysis in Section 3, there is a contradiction in the criterion for the choice of the map parameter L. In order to get a better solution as $r\to\infty$, the larger L is needed. While for the sake of the computational cost, the smaller L is demanded. The effect of the map parameter L on the amplification as functions of k and Re is plotted in Figures 4 and 5. It shows that the largest amplification for various k and Re takes place under the condition that L is about 3. We adopted the map parameter values with $L=3$ for the main calculation; this value represents the best compromise between the competing demands of the accuracy and the cost of the computation.

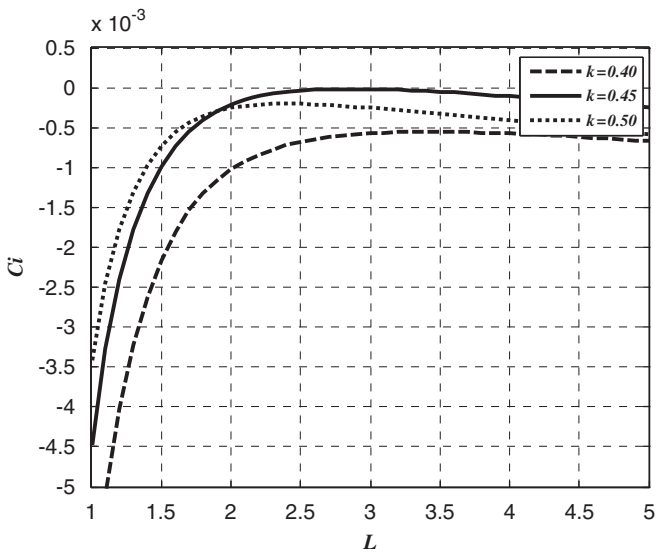

Figure 4. The effect of map parameter L on amplification factor with various k for fixed $Re=37.7$.

DOI: 10.1002/fld

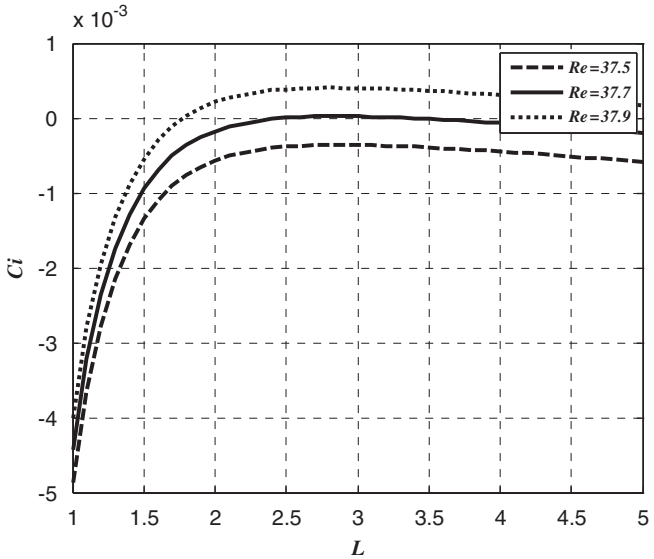

Figure 5. The effect of map parameter L amplification factor with various Re for fixed $k=0.45$.

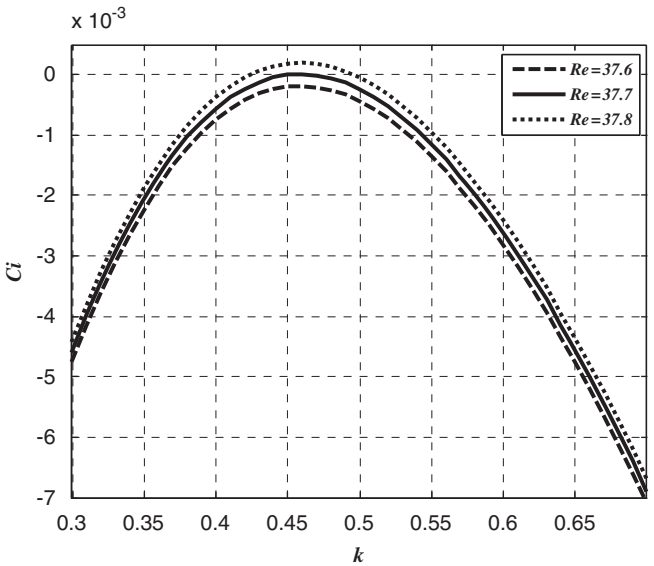

Figure 6. Amplification factor as a function of Re and k.

5.3. The critical Reynolds number

To obtain the critical Reynolds number, the amplification factor for some values of Re close to the critical Reynolds number is plotted in Figure 6. The critical Reynolds number is the point where

DOI: 10.1002/fld

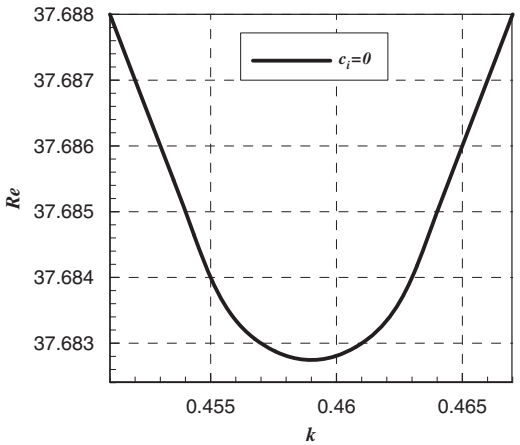

Figure 7. The neutral curve in $k-Re$ plane of round jet for $n=1$ mode.

Table I. Comparison of critical Reynolds number for $n=1$ mode.

Reference	Re	k	c_r
Morris [31]	37.64	0.44	0.1
Lessen and Singh [32]	37.9	0.3989	0.08
Salgado and Sandham [30]	37.8	0.417	0.09
Kulkarni and Agarwal [5]	37.68	0.4505	0.104
Xie *et al.* [24]	37.89	0.45	0.103
Present	37.6828	0.459	0.103

the curve $c_i(k)$ becomes tangent to the $c_i=0$ line. And in $k-Re$ plane the neutral curve ($c_i=0$ line) separates the space into two zones: one is stable and the other is unstable, which is shown in Figure 7.

From the graph the critical Reynolds number is found to be 37.6823 and the corresponding wavenumber is 0.459 for $n=1$ mode; under these conditions, the amplification is $c_i=-1.199819562286690\text{e}-006$. The present result is also compared with some of the other values reported by researchers in Table I.

6. CONCLUSION

The incompressible linear stability equations for a round jet in cylindrical polar coordinates with Petrov–Galerkin spectral method have been presented. To construct a basis function set for the unbounded domains, it is necessary to assume the asymptotic behavior of the approximated functions for large r. We conclude from the examples given above that mappings are an effective way to solve problems in infinite domains provided that the solution is simple at infinity. When mappings are applicable, the proper choice of mapping should be based on the criterion that the

DOI: 10.1002/fld

solution to the problem is be smooth in the mapped coordinate and incorporate the treatment of the singularity. For linear stability of a round jet, the exponential mappings is favorable.

Problems posed in (r, θ) polar coordinates can be solved efficiently by spectral methods by using a Chebyshev discretization for r and a Fourier discretization for θ. To weaken the coordinate singularity at $r=0$, one approach is to take $x \in [-1, 1]$ instead of $x \in [0, 1]$. The numerical simulation was performed by a Matlab code similar to that of Meseguer and Trefethen [23]. The critical Reynolds number is also computed and shown to be in good agreement with those reported in the literature. The method is validated against the results with a fifth-order Runge–Kutta method [5], compact FD method [30] and domain truncation method [24].

ACKNOWLEDGEMENTS

This work is supported by the National Natural Science Foundation of China (Grant No. 50806023) and the National Natural Science Foundation of China (Grant No. 10632070) and the National Natural Science Foundation of China (Grant No. 50721005). The authors would like to thank the valuable discussions and suggestions from *Dr F. B. Bao* in *Zhejiang University* for the development of the present work.

REFERENCES

1. Rayleigh L. On the stability or instability of certain fluid motions. *Proceedings of the London Mathematical Society* 1880; **11**:57–70.
2. Schmid PJ, Henningson DS. *Stability and Transition in Shear Flows*. Springer: Berlin, New York, 2000.
3. Drazin PG, Reid WH. *Hydrodynamic Stability* (2nd edn). Cambridge University Press: Cambridge, 2004.
4. Lewis HR, Bellan PM. Physical constraints on the coefficients of Fourier expansions in cylindrical coordinates. *Journal of Mathematical Physics* 1990; **31**(11):2592–2596.
5. Kulkarni TM, Agarwal A. Viscous linear instability of an incompressible round jet. *ISVR Report No. 317*, 2007.
6. Batchelor GK, Gill AE. Analysis of the stability of axisymmetric jets. *Journal of Fluid Mechanics* 1962; **14**:529–551.
7. Mohseni K, Colonius T. Numerical treatment of polar coordinate singularities. *Journal of Computational Physics* 2000; **157**:787–795.
8. Canuto C, Hussaini MY, Quarteroni A, Zang T. *Spectral Methods in Fluid Dynamics*. Springer: Berlin, New York, 1988.
9. Matsushima T, Marcus PS. A spectral method for polar coordinates. *Journal of Computational Physics* 1995; **120**:365–374.
10. Quartapelle L, Verri M. On the spectral solution of the three-dimensional Navier–Stokes equations in spherical and cylindrical regions. *Computer Physics Communication* 1995; **90**:1–43.
11. Chen HL, Su YH, Shizgal BD. A direct spectral collocation Poisson solver in polar and cylindrical coordinates. *Journal of Computational Physics* 2000; **160**:453–469.
12. Lopez JM, Marques F, Shen J. An efficient spectral projection method for the Navier–Stokes equations in cylindrical geometries. *Journal of Computational Physics* 2002; **176**:384–401.
13. Huang W, Sloan DM. Pole condition for singular problems: the pseudo spectral approximation. *Journal of Computational Physics* 1993; **107**:254–261.
14. Fornberg B, Sloan DM. A review of pseudospectral methods for solving partial differential equations. *Acta Numerica* 1994; **3**:203–267.
15. Fornberg B. A pseudospectral approach for polar and spherical geometries. *SIAM Journal on Scientific Computing* 1995; **16**:1071–1081.
16. Marques F, Mercader I, Batiste O, Lopez JM. Centrifugal effects in rotating convection: axisymmetric states and three-dimensional instability. *Journal of Fluid Mechanics* 2007; **580**:303–318.
17. Lopez JM, Marques F, Mercader I, Batiste O. Onset of convection in a moderate aspect-ratio rotating cylinder: Eckhaus–Benjamin–Feir instability. *Journal of Fluid Mechanics* 2007; **590**:187–208.
18. Lopez JM, Cui YD, Marques F, Lim TT. Quenching of vortex breakdown oscillations via harmonic modulation. *Journal of Fluid Mechanics* 2008; **599**:441–464.

DOI: 10.1002/fld

19. Mercader I, Alonso A, Batiste O. Spatiotemporal dynamics near the onset of convection for binary mixtures in cylindrical containers. *Physics Review E* 2008; **77**:036313.
20. Priymak VG. Pseudospectral algorithms for Navier–Stokes simulation of turbulent flows in cylindrical geometry with coordinate singularities. *Journal of Computational Physics* 1995; **118**:366–411.
21. Priymak VG, Miyazakiy T. Accurate Navier–Stokes investigation of transitional and turbulent flows in a circular pipe. *Journal of Computational Physics* 1998; **142**:370–411.
22. Lopez JM, Shen J. An efficient spectral projection method for the Navier–Stokes equations in cylindrical geometries I. Axisymmetric cases. *Journal of Computational Physics* 1998; **139**:308–326.
23. Meseguer A, Trefethen LN. Linearized pipe flow to Reynolds number 10^7. *Journal of Computational Physics* 2003; **186**:178–197.
24. Xie ML, Lin JZ, Zhou HC. Viscous linear instability of an incompressible round jet with Petrov–Galerkin spectral method. *Theoretical and Computational Fluid Dynamics*, submitted.
25. Grosch CE, Orszag SA. Numerical solution of problems in unbounded regions: coordinate transformations. *Journal of Computational Physics* 1977; **25**:273–296.
26. Boyd JP. *Chebyshev and Fourier Spectral Methods* (2nd edn). Springer: Berlin, 1999.
27. Matsushima T, Marcus PS. A spectral method for unbounded domains. *Journal of Computational Physics* 1997; **137**:321–345.
28. Spalart PR, Moser RD, Rogers MM. Spectral methods for the Navier–Stokes equations with one infinite and two periodic directions. *Journal of Computational Physics* 1991; **96**:297–324.
29. Moser RD, Rogers MM. The three dimensional evolution of a plane mixing layer: paring and transition to turbulence. *Journal of Fluid Mechanics* 1993; **247**:275–320.
30. Salgado AD, Sandham ND. Viscous instability of a compressible round jet. *ISVR Report No. AFM-07/1*, 2007.
31. Morris PJ. The spatial viscous instability of axisymmetric jet. *Journal of Fluid Mechanics* 1976; **77**:511–529.
32. Lessen M, Singh PJ. The stability of axisymmetric free shear layers. *Journal of Fluid Mechanics* 1973; **60**: 433–457.
33. Gottieb D, Orszag SA. *Numerical Analysis of Spectral Methods*: *Theory and Applications*. SIAM: Philadelphia, PA, 1977.

DOI: 10.1002/fld